Bio-inspired stimuli-responsive materials

Prof. Dr. C. Weder

Adolphe Merkle Institute and National Competence Center in Research Bio-Inspired Materials, University of Fribourg, Chemin des Verdiers 4, CH-1700 Fribourg

The National Center of Competence in Research (NCCR) Bio-Inspired Materials was launched in June 2014 to coordinate and promote research, education, and innovation in the domain of “smart” bio-inspired materials. The Center’s research takes inspiration from natural materials to establish design rules and strategies for the creation of macromolecular and nanomaterial-based building blocks and their assembly into complex, hierarchically ordered stimuli-responsive materials with new and interesting properties. Another objective is to develop an understanding for the interactions of such materials with living cells and use the generated knowledge to develop innovative applications. In this presentation an overview of the Center and its various activities will be given and several recently developed materials platforms will be discussed, including mechanically responsive and mechanically adapting polymer systems, bio-inspired optical materials, and hierarchically structured nanomaterials for biomedical applications.

Bone growth and regeneration – A materials science perspective

Prof. Dr. P. Fratzl

Max Planck Institute of Colloids and Interfaces, Department of Biomaterials, Potsdam, Germany

Our skeleton needs to carry the body weight and to resist mechanical impacts. This capability or, conversely, bone fragility are controlled by the amount of bone mass, the shape and internal architecture of the bones, as well as by the material of which they are built. Bone material consists of a complex multi-scale arrangement of mineralized collagen fibrils containing mineral, water, proteoglycans as well as some non-collagenous proteins. This organization is by no means constant during our life time. It changes with growth and bone maturation, but even adult bone is constantly remodeled and, thus, able to repair damaged tissue and to adapt to the loading situation. In preventing fractures, the most important mechanical property is toughness, which is controlled primarily by the intricate multi-scalar fiber arrangement of the tissue that develops during bone formation and maturation. However, how this complex structure is controlled and adapted through the action of bone forming cells remains a mystery. The talk will address recent in-vitro and ex-vivo experiments of bone tissue formation and regeneration that shed some light on this issue.

3D Printing of biologically-inspired materials

Prof. Dr. A. R. Studart

Complex Materials, Department of Materials, ETH Zurich, 8093 Zurich, Switzerland

Biological materials exhibit heterogeneous architectures that are tuned to fulfill the functional demands and mechanical loading conditions of their specific environment. Examples range from the cellulose-based organic structure of plants to collagen-based skeletal parts like bone, teeth and cartilage. Because they are often utilized to combine opposing properties such as strength and low-density or stiffness and wear resistance, the heterogeneous architecture of natural materials can potentially address several of the technical limitations of artificial implants or composites in general. However, current man-made manufacturing technologies do not allow for the level of composition and fiber orientation control found in natural heterogeneous systems. In this talk, I will show that 3D printing and additive manufacturing routes offer an exciting pathway for the fabrication of biologically-inspired materials with unprecedented heterogeneous architectures and functional properties.

Novel hyaluronan-based hydrogels to support endogenous cartilage repair

M.L. Vainieri[1,2], K. Sivasubramaniyan[2], A. Lolli[2], D. Eglin[1], A. Yayon[3], E. Wexselblatt[3], M Alini[1], S Grad[1], G Van Osch[2]

[1]AO Research Institute, Davos Platz, Switzerland. [2] Department of Orthopedics and Otorhinolaryngology, Erasmus MC, University Medical Centre, Rotterdam, The Netherlands, [3]Procore Laboratories, Nes Ziona, Israel

INTRODUCTION: Endogenous cartilage repair strategies aim to recruit endogenous mesenchymal stem cells (MSCs) to injuries, subsequently inducing *in situ* chondrogenesis. A major challenge is the design of a microenvironment promoting MSCs differentiation. Hyaluronan-based hydrogels are suitable biocompatible materials commonly used in cartilage tissue engineering. With the aim to select the most promising hydrogel, we investigated the ability of Hyaluronic Acid (HA)-Fibrin and HA-Tyramine hydrogels to support MSCs migration, ingrowth and differentiation *in vitro* and *in vivo*.

METHODS: Spheroids of 500 CFDA-SE-labelled bone marrow hMSCs from 3 donors were formed. The spheroids were embedded in HA-Fibrin and HA-Tyramine hydrogels with three crosslink densities as controlled by H_2O_2 concentration, 150, 300 and 600µM respectively. Cultures with/ without the chemotactic factor, PDGF-BB (50ng/ml) were performed. Migratory area of the cells from the core was measured by microscopy. For invasion assays, free-floated hydrogels were cultured for 7 days in α-MEM, 1% ITS with hMSCs in suspension. Chondrogenesis of hMSCs in the hydrogels[1, 2] was confirmed by qRT-PCR and histology after culture in chondrogenic medium for 28 days. Osteochondral defects made in bovine osteochondral biopsies[3] were filled with HA-Fibrin and HA-Tyramine (150µM H_2O_2) hydrogels with/without PDGF-BB (1µg/ml)[4] and subcutaneously implanted in athymic mice for 4 weeks. Histological sections were stained with thionine.

RESULTS: HA hydrogels allowed cell migration from the spheroids in presence of PDGF-BB, inducing progressive increase over three days culture. HA-Tyramine gels with the lowest crosslinking densities (150µM H_2O_2) were softer and promoted faster migration than stiffer gels. HA-Fibrin supported the broadest cells migration area (5-fold increase compared to HA-Tyramine hydrogels). When hMSCs were cultured in suspension with floated gels, cells infiltrated the hydrogel within 7 days, but no significant differences were detectable in presence or absence of PDGF-BB. Both hydrogels supported *in vitro* hMSCs chondrogenesis, as shown by collagen II and aggrecan expression and glycosaminoglycan production. *In vivo*, HA-Fibrin and HA-Tyramine with or without PDGF-BB favored endogenous cell invasion and cartilage production within 4 weeks. These processes were better supported in HA-Fibrin compared to HA-Tyramine hydrogels (Fig.1).

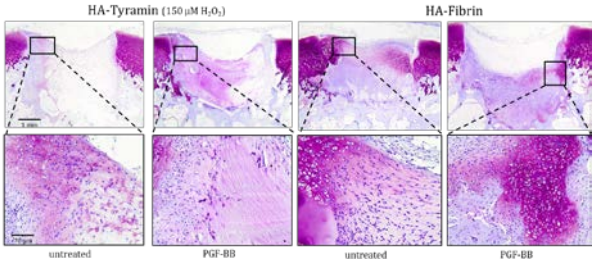

Figure 1. Endogenous cells recruitment and differentiation in vivo. Thionine staining (pink=GAGs) of osteochondral defect biopsies filled with HA-Tyramine and HA-Fibrin hydrogels with/without PDG-BB after 4 weeks implantation. Dashed lines indicate x4 the original magnification. Scale bars 1mm and 70µm.

DISCUSSION & CONCLUSIONS: HA-Fibrin hydrogel is the most favorable matrix, which permit MSCs infiltration and new matrix formation *in vivo*-, even in absence of a chemotactic stimulus, such as PDGF-BB. Our system can be employed for delivering chemoattractants to enhance cartilage repair by endogenous stem cells.

ACKNOWLEDGEMENTS: This project has received funding from the European Union's Horizon 2020 research and innovation programme under Marie Sklodowska-Curie Grant Agreement No 642414.

Fractionated human adipose tissue as a native biomaterial for the generation of a bone organ by endochondral ossification

J. Guerrero[1], S. Pigeot[1], J. Müller[1], D.J. Schaefer[2], I. Martin[1], A. Scherberich[1,2]

[1] University of Basel Hospital, Department of Biomedicine, Tissue Engineering, Basel, Switzerland. [2] University Hospital of Basel, Department of Plastic, Reconstructive, Aesthetic and Hand Surgery, Switzerland

INTRODUCTION: Many steps are required to generate bone through endochondral ossification with adipose mesenchymal stromal cells (ASC), from cell isolation to *in vitro*, monolayer expansion, seeding into scaffolds and cartilaginous differentiation. Moreover, monolayer expansion and passaging of ASC strongly decreases their differentiation potential. Here, we proposed a novel approach based on adipose tissue as scaffold with cell expansion, matrix formation and chondrogenic differentiation directly inside native adipose tissue.

METHODS: Human liposuctions were fractionated as previously described and cultured in suspension to allow ASC expansion. After 3 weeks, 4-mm cylinders were punched out of the resulting constructs (named Adiscaf) and cultured for 4 weeks with chondrogenic induction medium and 2 more weeks with hypertrophic induction medium. Minimally monolayer expanded ASC from the same donors, seeded in 4-mm cylinders of collagen sponge (Ultrafoam™) and cultured with the same differentiation media were used as control. Both constructs types were then implanted subcutaneously in nude mice for 8 weeks.

RESULTS: At the end of the proliferation phase (3 weeks), cells in Adiscaf had proliferated and generated a stromal matrix containing ASC as well as endothelial cells. After the chondrogenic phase (4 weeks), Adiscaf produced cartilage, containing high levels of glycosaminoglycans and type II collagen. Upon hypertrophic culture, gene and protein expression analyses showed upregulation of markers of terminal chondrogenic differentiation, as type X collagen. Adiscaf showed superior *in vitro* differentiation as compared to the standard paradigm involving isolation and monolayer expansion of ASC (*Fig. 1*).

In vivo, after 8 weeks of implantation, Adiscaf resulted in ectopic bone tissue formation in comparison to the same donor's cells seeded inside Ultrafoam. Adiscaf constructs generated bone tissue, both of cortical and trabecular types, vascularized and included a bone marrow compartment.

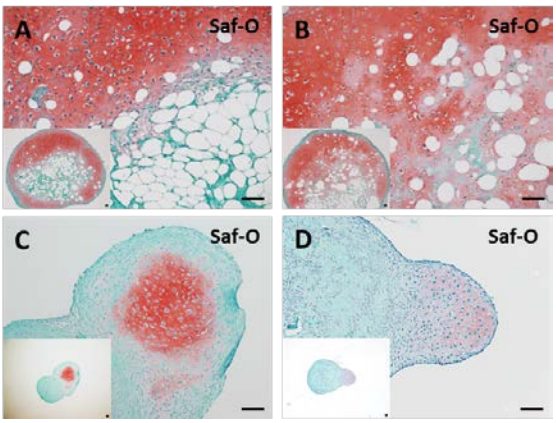

Fig. 1: (A-D) Safranin-O staining of chondrogenic (4 weeks) Adiscaf (A) and Ultrafoam (C) scaffold-based samples and hypertrophic (4 + 2 weeks) Adiscaf (B) and Ultrafoam (D) scaffold-based samples. Scale bar = 100 µm. Abbreviations : Saf-O, Safranin-O.

DISCUSSION & CONCLUSIONS: We showed that our new paradigm exploit the physiological niche of adipose tissue in order to better maintain the functionality of cells within the adipose tissue during their *in vitro* expansion. This study demonstrates that adult human adipose tissue used as a native construct can generate a cartilaginous engineered tissue *in vitro* and a bone organ by endochondral ossification after *in vivo* implantation, introducing a novel concept in the generation of osteogenic grafts for bone repair.

ACKNOWLEDGEMENTS: This study was supported by the Swiss National Science Foundation, SNF grant # 310030-156291 (to A.S. and I.M.).

Genipin-enhanced fibrin hydrogel combined with engineered silk composite for intervertebral disc repair

D.A. Frauchiger[1], R.D. May[1], M. Wöltje[2], L.M. Benneker[3], B. Gantenbein[1]

[1] Tissue and Organ Mechanobiology, Institute for Surgical Technology and Biomechanics, University of Bern, Switzerland, [2] Institute of Textile Machinery and High Performance Material Technology, TU Dresden, Germany, [3] Department of Orthopaedic Surgery, Inselspital, Switzerland

INTRODUCTION: Low back pain caused by the intervertebral disc (IVD) is an increasing problem without satisfactory treatment option. Hence, we aim for an "inside-out" approach for repairing herniated IVDs or injuries of the outer annulus fibrosus (AF) by using a fibrin hydrogel in combination with engineered silk. For doing so, we investigated *in vitro* and *ex vivo* organ culture the feasibility of genipin cross-linked fibrin in combination with an engineered silk composite.

METHODS: Fresh coccygeal bovine IVDs were isolated under aseptic conditions, and a 2mm biopsy punch was used to induce a circular injury. The injury was filled with genipin-enhanced human-based fibrin hydrogel (Tisseel, Baxter). To seal the AF, a GMP-compliant silk membrane-fleece composite was placed on the hydrogel-filled cavity, Fig. 1A. Immediately after repair, IVDs were subjected to *in vitro* organ culture for 14 days using either one of the three loading regimes: 1) complex: 0.2MPa compression and 0±2° torsion at 0.2Hz for 8h/day, 2) static diurnal: 0.2MPa compression for 8h/day, 3) no loading,

To achieve complex loading, a custom-built two-degree of freedom bioreactor was used.

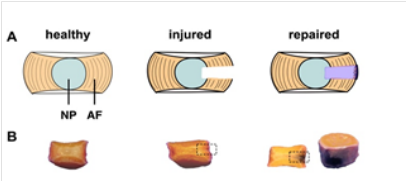

*Fig.1: **A** Drawing of healthy disc, injury induced by biopsy punch and repaired disc with hydrogel and silk composite. **B** Macroscopic pictures of IVDs after 14 days of no loading culture. Blue discoloration of repaired disc arises from genipin.*

Measured end-point parameters were inspection for seal failure (herniation), disc height, metabolic activity (resazurin sodium salt assay), DNA, glycosaminoglycan (GAG) contents and gene expression of major IVD genes. Additionally, histology was performed to visualize injury and integration of hydrogel and silk. Furthermore, cytocompatibility of genipin was tested *in vitro* with low-passage human mesenchymal stem cells (MSC, n=6) and donor matched (n=3) human AF and nucleus pulposus (NP) cells. Culture medium with increasing genipin concentrations and DMSO only as control were cultured with 120,000 cells/well (48-well plate) for 14 days, media was exchanged every 2-3 days. Mitochondrial activity (resazurin salt) was investigated on day 1, 4, 7 and 14.

RESULTS: No herniation of repaired discs could be observed throughout 14 days of culture. The genipin-enhanced fibrin hydrogel was capable of holding the silk composite in place, Fig. 1B. Repair of discs did not lead to a restoration of disc height. Nevertheless, metabolic activity, DNA/GAG content and disc height of repaired discs did not differ significantly from the IVDs. Except higher DNA content under static loading for the repaired discs compared to the injured IVDs (p-value ≤ 0.004). *In vitro* experiments on the cellular level showed barely any cell activity for the cells treated with genipin. Genipin showed high cytotoxicity *in vitro* on cells tested by reducing the mitochondrial activity to zero.

DISCUSSION & CONCLUSIONS: Genipin-enhanced fibrin hydrogel in combination with silk composite was able to form a durable AF seal that withstood instant loading. Nevertheless, our *in vitro* cytocompatibility test on primary MSC, AF and NP cells suggests a strong cytotoxic effect of genipin. The future challenge is now to identify a less toxic but still mechanically load bearing hydrogel for AF repair.

ACKNOWLEDGEMENTS: This project was funded by the Gebert Rüf Stiftung project #GRS-028/13. We thank Eva Roth for her valuable assistance in cell isolation, histology and biochemical assays. We further thank Jochen Walser for assistance with the bioreactor.

Designing synthetic photo-clickable hydrogels to direct cell fate

X-H.Qin[1], X. Wang[2], M. Rottmar[1], B. Nelson[2], K. Maniura-Weber[1]

[1]Biointerfaces, Empa - Swiss Federal Laboratories for Materials Science and Technology, St Gallen, CH. [2] Multiscale Robotics, ETH Zürich, CH

INTRODUCTION: Nature has designed fibrin as a functional matrix in wound healing that directs cell-matrix remodelling in space and time to form de novo tissues. Synthetic gels have been used for 3D cell culture to study how cells sense and respond to their 3D environments. Despite remarkable progress, precise control of cell fate in a 3D matrix remains challenging. Here, we present a robust photo-clickable hydrogel composed of protease-sensitive polyvinyl alcohol (PVA) matrices. Using two-photon micropatterning, we demonstrate that cell function can be controlled at high spatial resolution via site-specific photo-grafting. Furthermore, this material enables two-photon lithography (TPL) of 3D complex objects at speeds as high as 50 mm/s.

METHODS: Norbornene-functionalized PVA (nPVA) was prepared as previously described. Degradable and non-degradable gels were prepared by photocrosslinking of nPVA with a di-cysteine peptide (KCGPQGIWGQCK) and dithiothreitol as the crosslinker at thiol-ene ratio of 4:10, and 1.0 mM CGRGDS. Photo-rheology was applied to assess gel mechanics and enzymatic degradation. Cytocompatibility was evaluated by live-dead and cell proliferation assay of photoencapsulated human dermal fibroblasts (HDFs). For laser-directed cell invasion, HDF clusters were first encapsulated in degradable, non-adhesive PVA gels (10 %) before transfer into photoinitiator solutions containing 1.0 mM CRRGDS. Two-photon micropatterning and TPL were performed on a LSM780 microscope and a Nanoscribe GT micro-printer, respectively.

RESULTS & DISCUSSION: PVA gels were rendered protease-degradable and adhesive by incorporating protease-sensitive peptide as the crosslinker and fibronectin-derived CGRGDS as the ligand. To investigate how matrix degradation effects on 3D cell growth, degradable and non-degradable PVA gels were prepared by UV photopolymerization (Scheme 1). We chose an off-stoichiometric thiol-ene polymerization to facilitate subsequent bio-functionalization with peptide motifs. Gel formation takes ca. 1 min irradiation as evidenced by photo-rheology. Cell viability in degradable gels is much higher than that in non-degradable gels. Furthermore, cells proliferate in degradable gels but not in non-degradable gels.

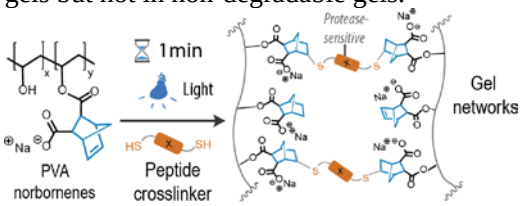

Scheme 1. Illustration of protease-sensitive PVA gel networks via off-stoichiometric thiol-ene photopolymerization.

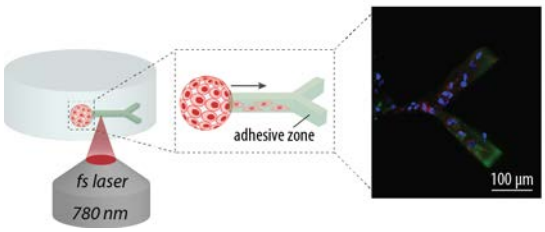

Figure 1. Illustrated directed cell invasion inside a 3D gel within a Y-shaped region and confocal image of the patterned region with cells inside.

The mesh size of PVA gels is ca.10 nm. Therefore, cell invasion in such matrices is limited to matrix degradation by cell-secreted proteases. This was proved by the addition of a broad spectrum protease inhibitor, which fully blocked cell invasion. Control experiments in degradable, non-adhesive gels show no cell invasion. These results show that cell invasion requires both proteolysis and adhesive ligands in order to clear out a path. To demonstrate directed cell invasion (Figure 1), adhesive peptides were site-specifically immobilized in PVA gels. Cells were found to be spatially refined in the patterned area.

CONCLUSIONS: In conclusion, we have developed a versatile hydrogel that is fully synthetic, modular and permissive for cell-matrix remodelling. With this platform, one can precisely study and manipulate 3D cellular environments on a two-photon microscope. This system holds promise for potential applications in the fields of 3D cell culture and tissue engineering.

Clinical relevant bioinks for enhanced cartilaginous matrix deposition

B. Kessel[1], G. Barreto[1], P. Guillon[1], M. Zenobi-Wong[1]

[1] *Tissue Engineering and Biofabrication Lab, Swiss Federal Institute of Technology in Zurich, Zurich, CH*

INTRODUCTION: Cartilage is a tissue with limited capabilities to regenerate damage and current treatments often have poor clinical outcome. New, cell-based therapies like autologous chondrocyte implantation (ACI) show promising results and are slowly becoming the new standard of care.
The objective of this project is to develop a personalized strategy for cartilage replacement. We 3D bioprint unmodified, FDA-compliant biopolymers and primary chondrocytes to produce cell-laden cartilage tissue grafts. Based on previous research done in our lab, we developed a novel bioink based on three components: alginate, gellan and hyaluronic acid (HA). Alginate is used as an easy crosslinking system while gellan gum introduces shear thinning and shear recovery properties to print with high shape fidelity. Hyaluronic acid as a native component of the extracellular matrix of cartilage improves the quality of the matured tissue graft.

METHODS: We encapsulated passage 2, primary bovine chondrocytes in two different bioinks (*Table 1*). Cell-laden, small cylinders (d=4mm, h=2mm) were printed and cultured with TGFβ1 supplemented media for up to 8 weeks. Printed tissue grafts were analysed by fluorescent live/dead viability staining, compression tests and immunohistochemical stainings.
Materials and bioinks were analysed for endotoxin release with HEK-Blue™ TLR4 cells. Ear-shaped scaffolds were 3D scanned after crosslinking and deformation was analysed with an in-house developed algorithm.

Table 1. Composition of used bioinks.

	Alginate	Gellan Gum	Hyaluronic Acid
Bioink	**2%**	**3%**	**-**
Bioink+HA	**1.5%**	**2.5%**	**1%**

RESULTS: Cells in Bioink+HA scaffolds showed significant higher viability as well as proliferation compared to cells in Bioink scaffolds after 8 weeks. (Viable cells Bioink: 68.0% ± 4.5, Bioink+HA: 92.6% ± 0.5, n=9, p<0.0001)

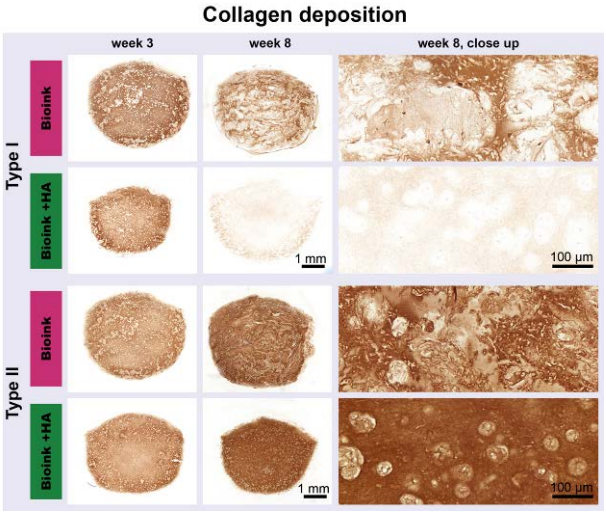

Figure 1: Histological comparison of collagen deposition in Bioink and Bioink+HA grafts.

Immunohistochemical analysis at week 3 revealed homogenous deposition of collagen I and II throughout the whole scaffolds for both bioinks *(Figure 1)*. At week 8 Bioink+HA showed a cartilage like microstructure with only minimal collagen type I staining.
Both bioinks, as well as component materials, triggered only minimal response (<0.1 ng/ml) in endotoxin sensitive cells.
Unlike ear grafts printed with Bioink, which exhibited strong longitudinal shrinkage and a loss of features, Bioink+HA grafts kept the proportion of the desired model.

DISCUSSION & CONCLUSIONS: The addition of HA to a bioink based on alginate and gellan gum results in a more homogenous ECM microstructure and a higher collagen II to I ratio. In addition it greatly reduces shape deformation and helps to preserve features in the printed scaffolds.
All materials used are FDA-approved and contain only minimal traces of endotoxins. These results would support the use of the Bioink+HA in clinical applications.

ACKNOWLEDGEMENTS: This work was supported by the Swiss National Science Foundation (Grant number: CR3213_166052).

Magnetic nanocomposite hydrogels combined with static magnetic field for enhanced bone regeneration

M. Filippi[1], B. Dasen[1], J. Guerrero[1], G. Born[1], M. Ehrbar[2], and A. Scherberich[1]

[1]*Department of Biomedicine, University Hospital Basel, University of Basel, Hebelstrasse 20, 4031,* [2] *Laboratory for Cell and Tissue Engineering, Department of Obstetrics, University Hospital Zurich, Zurich, Switzerland.*

INTRODUCTION: The activation of the mechanotransduction signaling pathways in the cells through the application of magnetic forces and magnetic nanoparticles (MNPs), known as "magnetic actuation", has been reported to induce stem cell differentiation towards the osteogenic lineage and enhance the endothelial organization during the vascular development. The stromal vascular fraction (SVF) derived from adipose tissue contains heterogeneous cell populations including mesenchymal stem cells and vascular progenitors. Here, we described novel MNP-dispersed hydrogels to magnetically stimulate SVF cells and obtain constructs for bone tissue engineering with enhanced osteogenic and vasculogenic potential.

METHODS: Magnetic gels were obtained by co-assembly of Polyethylene glycol (PEG)-based hydrogels with superparamagnetic iron oxide nanoparticles (SPIONs, 10 nm radius) and freshly isolated SVF cells (6.0×10^6/ml). Gels were stimulated for 2 weeks by exposure to 50 mT neodymium magnets applied under the culture wells, either with or without osteogenic differentiation factors. Structural and biological characterization of gels was carried out by scanning electron microscopy (SEM), histological or immunohistochemical imaging of sections, confocal microscopy, protein and gene expression analysis of osteogenic and vascular markers and genes acting as key regulators of the mechanotransduction signalling pathways. Finally, through subcutaneous transplantation in immunodeficient mice, the bone formation and vascularization were analysed after 1 and 8 weeks *in vivo* by µCT and histology.

RESULTS: After homogeneous assembly of all the construct components, the SPIONs migrated through the gel following the magnetic gradient, being completely released from the constructs after 9 days. The magnetically actuated cells displayed incremented metabolic activity, matrix production and mineralization, as shown by histology and SEM. After 1 culture week, overexpression of osteogenic markers (i.e. Runx2, Col I, Osterix, ALP) and increased ALP enzymatic activity were found with respect to control gels cultured into osteogenic medium without magnetic actuation. After 2 weeks, magnetized gels showed large $CD31^+$ endothelial populations, clustering zones of elongated aligned cells and consistent production of soluble VEGF. Endothelial, pericytic and perivascular genes (CD31, SMA, TCAD, NG2, VEGFα), and genes commonly involved in the mechanotransduction pathways (Integrins and MAPK pathway effectors) were overactivated. Enhanced vascularization and mineralization were retained *in vivo*, as demonstrated by increased expression of vascular markers and generation of more compact and structured bone-like material.

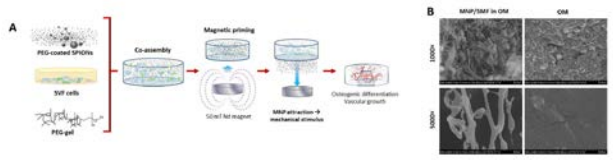

Fig. 1: A. Experimental scheme for magnetized gel generation and assessment of their biological effect. B. Cell morphology and extracellular matrix observed by SEM of magnetically actuated hydrogels (MNP/SMF in OM) as compared to unstimulated controls (OM).

DISCUSSION & CONCLUSIONS: We demonstrated that the exposure of the magnetized gels to a static magnetic field activates panels of osteo and vasculogenic marker genes, showing gross phenotypic signatures such as increased mineralization degree, and more advanced endothelial organization. The underlying mechanism is most likely to be ascribed to the mechanical stimulation on SVF cells operated by the SPION movement through the gel. We conclude that the present biomaterial retains a considerable potential as *in vitro* priming strategy for innovative tissue interfaces dedicated to efficient bone tissue engineering.

3D-printed auxetic structures for bio-medical application

F. Schuler[1], P. Renaud[2], M. de Wild[12]

[1]*Institut für Medizinaltechnik und Analysetechnik, School of Life Sciences, FHNW.* [2] *AVR - ICube, INSA Strasbourg.*

INTRODUCTION: The SPIRITS Interreg project (Smart Printed Interactive Robots for Interventional Therapy and Surgery) aims at developing innovative robotics by 3D-printing for interventional radiology and image guided surgery. In this context, the development of a pneumatic actuator is required to propel a biopsy needle also on different surgical tools. Beside the technical functionality and medical requirement of the OR environment, the component has to be optimised for undisturbed interaction with the used imaging technology. Based on a preceding project by INSA Strasbourg, the development of a metal-based, auxetic actuator is investigated for optimized translation performance

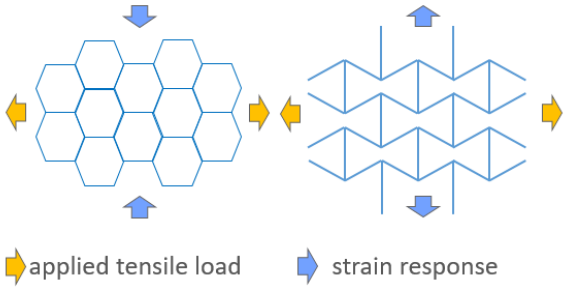

Fig. 1: Visualization of auxetic behavior (left) compared to standard material (right).

METHODS: SolidWorks™ (Dassault Systèmes, France) was used for the design and Magics™ (Materialise, Leuven, Belgium) for processing, slicing and support generation. The Selective Laser Melting (SLM) system (DMG Mori, former Realizer, Germany) is used as manufacturing process operating the machine models SLM-100 and SLM-125. The used materials are Ti grade 2 and a NiTi shape memory alloy. Process parameters for Ti were slightly modified standard parameters, NiTi parameters were based on. Mechanical testing was done using a hydropulser LFV-5-PA/EDC120 from Walter & Bai, W+B testing equipment.

RESULTS: It was possible to print auxetic structures down to a planned strut size of 300 µm. that had an elastic range of almost 10% and showed no critical failure in tensile tests up to 33% forced elongation. Furthermore, the mechanical properties of the structure (i.e. the spring constant) could be maintained almost constant (± 5%) despite the plastic deformation during the tensile test (compare Fig. 2).

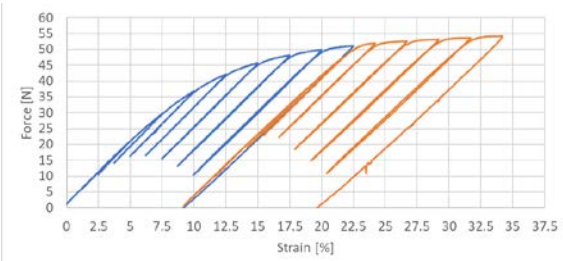

Fig. 2: Two consecutive tensile test of an auxetic structure, showing constant stiffness.

In stress-controlled cyclic loading tests at approximately 66% of their elastic limit, the samples failed after 40-50 k loading cycles. The critical failures were always preceded by defects in single elements.

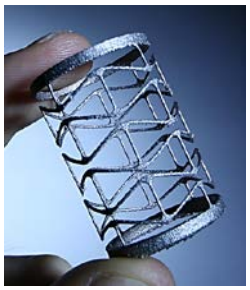

Fig. 3: 3D-printed auxetic Ti structure

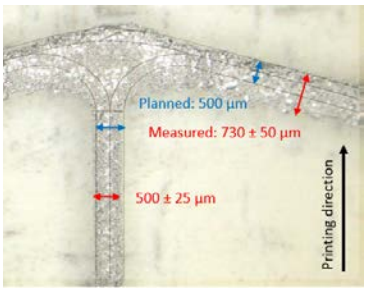

Fig. 4: Sintering of powder on down-facing surfaces

The construction of a functional actuator was not yet possible, due to the still relative stiff structures obtained. One reason for this is the thicker than planned structure, due to sintering of surrounding powder onto the printed structure (Fig. 4).

DISCUSSION & CONCLUSIONS: These initial mechanical results are quite promising, but further optimisation of the manufacturing process (e.g. energy input) is a necessity until thinner and still functional structures are obtained.

Novel patient specific implant for orbital floor repair using osteoinductive biomaterials

O. Guillaume[1], M. Geven[2], T. Schmid[1], D. Grijpma[2], R.R.M. Bos[3], R.G. Richards[1], M. Alini[1] and D. Eglin[1]

[1]AO Research Institute, AO Foundation, Davos, CH, [2] Department of Biomaterials Science and Technology, University of Twente, Enschede, NL, [3] University and University Medical Center Groningen, Groningen, NL

INTRODUCTION: Orbital floor (OF) fractures are commonly treated by implanting either bioinert titanium or by autologous grafts. As alternative, we introduce a personalized implant made of poly(trimethylene carbonate) loaded with hydroxyapatite (PTMC-HA). The implant is produced using stereolithography (SLA) based on patient CT scan. In this preclinical study, we validated the workflow for the production of personalized PTMC-HA implants and assessed their performance compared to standardized titanium implants in a repair OF defect on a sheep model.

METHODS: Implants fabrication was done using SLA of photo-crosslinkable PTMC mixed with HA. Preclinical study: (sheep n=12, ethic number 34_2016) was conducted by first scanning the OF bone of each sheep in order to design and to fabricate patient specific implants (PSI) made of PTMC-HA. The fabricated PSI was implanted after creating OF defect. Bone formation and defect healing was compared to manually shaped titanium mesh using time-laps X-ray analyses and histology (Giemsa-Eosin staining) over 3-months. Additionally, the osteoinductive property of the biomaterials was assessed by intramuscular implantation (IM).

RESULTS & DISCUSSION: In this study, we validated the possibility to produce PSI using a photo-crosslinkable resin based on PTMC and HA. SLA-fabricated PTMC-HA implants have a good shape fidelity (compared to the virtual implant), possess suitable mechanical stability to support tissues without provoking any eye displacement and exhibit a better bone integration compared to the standard material titanium mesh.

CONCLUSIONS: This study opens the field of patient-specific implants made of degradable and osteoinductive scaffolds fabricated using additive manufacturing to replace advantageously autologous bone and titanium implants in craniomaxillofacial surgeries.

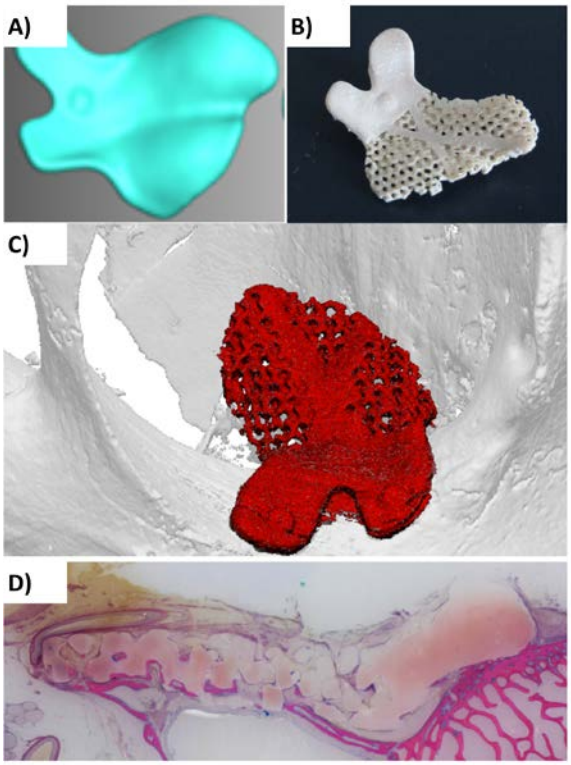

Figure 1: Virtual implant reproducing OF anatomy of a sheep (A) and SLA-produced equivalent (B). Following surgery, the implants were monitored using tomography (C) and bone ingrowth was assessed post-euthanasia using histology (G&E staining, D) showing in pink the bone tissue penetrating the porosity of the implant.

ACKNOWLEDGEMENTS: NSFC-DG-RTD Joint Scheme (Project No. 51361130034) and the European Union's 7th Framework Program under grant agreement n° NMP3-SL-2013-604517.

In vitro and *in vivo* study of the efficiency of a TGFβ1-loaded hyaluronan-based scaffold for cartilage tissue engineering

C. Levinson[1], E. Cavalli[1], N. Broguiere[1], A.L. Applegate[2], M. Zenobi-Wong[1]

[1]Tissue Engineering + Biofabrication Lab, ETH Zürich, CH. [2] Connective Tissue Biology Labs, School of Biosciences, CHUV Lausanne, CH

INTRODUCTION: Growth factors (GF) such as TGFβ1 play a crucial role in initiating and maintaining chondrogenesis. However little is known about their optimal dose and release profile for cartilage tissue engineering. Moreover GFs are potent molecules that can trigger unwanted side effects when released from the scaffold in an uncontrolled manner. Our aim is thus to develop a TGFβ1-loaded scaffold allowing its sustained release and ensure the safety and efficiency of the obtained tissue-engineered product.

METHODS: Hyaluronan-Transglutaminase gels (HA-TG) were obtained by modifying high molecular weight hyaluronan with two different fibrinogen-derived peptides, which can be crosslinked by the transglutaminase FXIII. Firstly, to avoid a burst release of TGFβ1, we covalently grafted heparin to HA-TG using the same chemistry (HA-Hep-TG) and measured the sustained release with ELISA (80 ng initially loaded, TGF concentration was determined for each supernatant uptake and cumulative amounts were plotted). Secondly, a dose screening to find the optimal concentration of GF was performed *in vitro* by loading various amounts of TGFβ1 in HA-Hep-TG gels, and subsequently looking at matrix deposition by encapsulated cells after 21 days of culture. The cells used were human chondroprogenitor cells (hCCs), mixed with the gel precursors prior to crosslinking. Thirdly, we tested the selected doses *in vivo* by implanting the scaffolds subcutaneously in nude mice for 6 weeks. Vessel ingrowth was monitored using photoacoustic imaging. Matrix production was assessed by histology and immunostaining.

RESULTS: HA-Hep-TG efficiently retained TGFβ1 in the scaffold since only 60% of the initial loaded amount was released from the gels after 2 weeks compared to 90% in the absence of heparin (Fig. 1 left). *In vitro*, the addition of Hep-TG to sustain TGFβ1 release led to similar matrix deposition compared to the addition of TGFβ1 in the medium, and the loading of TGFβ1 in the gel without Hep-TG led to almost no matrix production (Fig. 1 right). *In vivo*, absence of Hep-TG led to more severe side effects such as hematomas and swelling at the site of implantation, compared to scaffolds with no sustained release. Vessel ingrowth was not detected in any of the conditions. Histological stainings did not show a difference between the loading strategies, contrary to what was observed *in vitro*, highlighting the limitations of *in vitro* studies to predict the effect of bioactive molecules *in vivo*. No clear difference was seen between the two TGFβ1 doses either (Fig. 2).

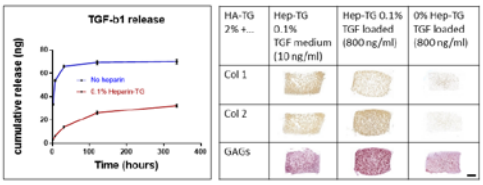

Fig. 1: Release profile of TGF-β1 (left) and in histology stainings of scaffolds cultured in vitro for 3 weeks. Scale bar: 1 mm.

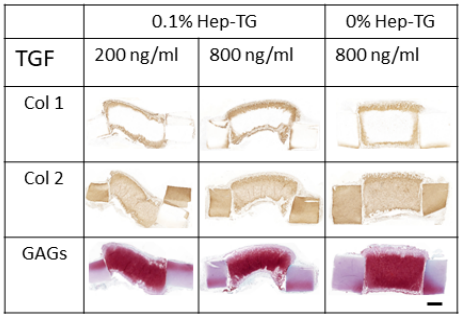

Fig. 2: Histology stainings of scaffolds in cartilage rings, implanted in vivo. Scale bar: 1 mm.

DISCUSSION & CONCLUSIONS: HA-Hep-TG shows high potential due to cartilaginous matrix deposition and limited side effects *in vivo*. The combination of hCCs and HA-TG also showed a potential due to the capacity of the cells to produce matrix *in vivo*, contrary to our observations *in vitro*. Ongoing long-term studies in mice and a pilot experiments in the sheep will give more information regarding the safety and efficacy of HA-TG loaded with TGFβ1, with or without Hep-TG to achieve a sustained release.

Extracellular matrix of engineered cartilaginous tissue as a scaffold material to induce chondrogenic differentiation

G. Lehoczky[1,2], F. Wolf[1], I. Martin[1], A. Barbero[1], K. Pelttari[1]

[1]Tissue Engineering Laboratory, Department of Biomedicine, University Hospital and University, Basel, Switzerland. [2] Department of Traumatology and Orthopedic Surgery, University Hospital Basel, Basel, Switzerland

INTRODUCTION: Extracellular matrix (ECM) from native (porcine/equine) articular cartilage has been shown to induce chondrogenic differentiation of mesenchymal stromal/progenitor cells (MSC) and de-differentiated articular chondrocytes (AC) *in vitro*. A similar capacity of human *tissue engineered* cartilaginous ECM (TEC-ECM), however, has not been investigated so far. We here asses the capability of TEC-ECM to promote/induce chondrogenic differentiation of different cell types, typically used or recently proposed for cell based cartilage repair, such as AC, MSC and nasal chondrocytes (NC).

METHODS: Cartilaginous tissues engineered culturing by expanded human NC in 3D pellet were lyophilised devitalised and pulverized to generate the TEC-ECM. Expanded NC (n=9 donors), AC (n=5) and bone marrow derived MSCs (n=2) were co-cultured with TEC-ECM for 21 days under standard chondrogenic differentiation condition but in the absence of the key chondrogenic factor TGFβ. The same cells were also cultured without TEC-ECM in pellets either with TGFβ (positive control) or without (negative control). The quality of the newly generated cartilaginous tissue was assessed histologically (SafraninO staining for glycosaminoglycans (GAG)) and the deposited cartilaginous matrix quantified biochemically, with the amount of initially applied GAG from the TEC-ECM subtracted. The fold-change in GAG deposition was determined for cells cultured with the TEC-ECM and the positive control cells in relation to the negative control cells cultured without TGFβ.

RESULTS: Histological analyses (Fig. 1) demonstrated that a cartilaginous tissue – with quality comparable to that of the positive control - was reproducibly generated by NC in the absence of TGFβ, when TEC-ECM was applied. No significant differences were observed in the increase of GAG deposition by NC with TEC-ECM (4.7±1.3-fold increase (mean±SEM) versus negative control) as compared to positive controls (11.3±5.8-fold). Also for AC and MSC, deposition of GAG was observed histologically and its increase quantified versus the negative control (2.3±0.5-fold and 3.1±0.7-fold, respectively), with no significant difference to corresponding positive AC (1.9±0.8-fold) and MSC controls (1.4-±0.2-fold).

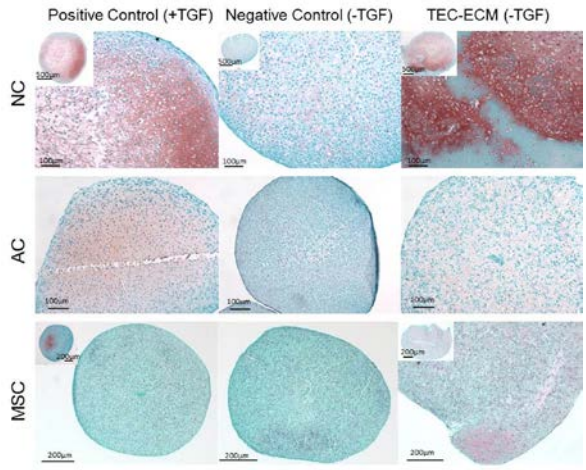

Fig. 1: Safranin O staining of NC, AC and MSC cultured with tissue engineered cartilaginous ECM with and without TGFβ.

DISCUSSION & CONCLUSIONS: We here demonstrate that application of ECM generated from tissue engineered cartilage can induce chondrogenic differentiation of different adult human primary cells. This indicates that bioactive components entrapped in the TEC-ECM can compensate and replace the typical chondrogenic growth factor TGFβ. Clinical application of this biomaterial could thus improve the capacity of the implanted cells and/or the progenitor cells resident in the joint (such as subchondral MSC), to regenerate the cartilage tissue. Which factors precisely are responsible for this chondro-inductivity, however, needs to be further investigated.

ACKNOWLEDGEMENTS: This work was funded by the SNSF grant 310030_149614.

Matrix topography and mechanical load mediate tendon fibroblast response to inflammatory signals

A.D. Schoenenberger[1,2], U. Silvan[1,2], S.F. Fucentese[1], J. Widmer[1,2], J.G. Snedeker[1,2]

[1] *University Hospital Balgrist, Zurich, Switzerland.* [2] *ETH Zurich, Zurich, Switzerland*

INTRODUCTION: The presence of immune cells in tendinopathic tissue and the impact of macrophage-secreted factors on the cellular response of primary human tendon fibroblasts (TFs) indicate a central role for inflammation in the regeneration of diseased tendon. In the present study we have used a recently developed *in vitro* model of tendon healing and early inflammation to analyze the impact of mechanical loading on TF response in terms of inflammatory pathway activation and anabolic/catabolic matrix activity.

METHODS: Primary human tendon fibroblasts were cultured on nanofiber polymer mats that structurally mimic either a healthy tendon matrix (aligned fibers) or a diseased matrix (randomly oriented fibers). Cells adhering to both substrate types were mechanically conditioned using a custom-made bioreactor by either static (0% strain) or cyclic (7% strain) loading for 24h (Fig. 1). After mechanical stimulation TFs were treated with 5 ng/ml IL1β for 15 min., and their response was assessed using qPCR against lineage-specific markers and a palette of matrix related genes. In addition, translocation of NFκB-p65 was quantified from fluorescent stained cells.

RESULTS: Quantification of cytoplasmic and nuclear levels of NFκB p65 subunit in TFs subject to cyclic loading revealed that mechanical stimulation significantly increased nuclear-translocation of p65 in TFs adhere to both substrate types, with more pronounced response on the randomly oriented fibers. Expression of tenogenic markers (*MKX*, *SCX*) remained at similar levels independently of the mechanical load. In turn, stimulation with the pro-inflammatory cytokine IL1β of TFs previously exposed to cyclic load displayed reduced p65 nuclear-translocation compared to the static load condition (Fig. 2C,D).

DISCUSSION: Matrix alignment and cyclic mechanical loading appear to cooperatively

mediate TF response to a pro-inflammatory stimulus. Our results support a plausible central role for these factors in certain vicious cycles of tendon disease. The controlled model we introduce provides first quantitative insight to mechanical regulation of tendon healing, which will likely be essential to the development of effective therapeutic strategies.

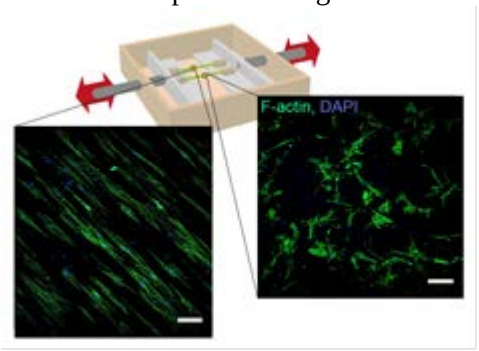

Fig. 1: Bioreactor model system. Fluorescent staining of nuclei (blue) and actin (green) of TFs. Cells were cultured on nanofiber polymer substrates that mimic healthy or disease matrix and were mechanically stimulated using a custom-made bioreactor (scale bar = 100 µm).

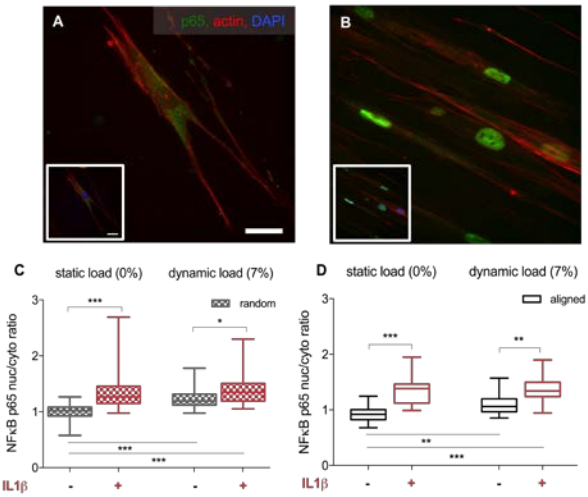

Fig. 2: TF response to mechanical loading and inflammatory signals. Immunofluorescent staining of the NFκB p65 subunit (green channel in A and B) and quantification of the cytoplasmic and nuclear fractions (TFs on random (C) and aligned substrates (D)). (n = 4,*P ≤ 0.05, **P ≤ 0.01,***P ≤ 0.001, scale bar = 20 µm.).

Cationic silica nanoparticle-based nanocomposite for bioprinting large tissue constructs with enhanced structural fidelity and mechanical strength

M. Lee, M. Zenobi-Wong

Tissue Engineering and Biofabrication Laboratory, Institute for Biomechanics, ETH Zürich, Zürich, CH

INTRODUCTION: Bioprinting is a promising technique for fabricating personalized tissue grafts as well as tissue-mimetic constructs. Hydrogel-based materials have been intensively studied as bioinks due to their excellent biocompatibility. However, intrinsic low mechanical strengths and swelling behaviours greatly hinder fabrication of tissue constructs with high structural fidelity and mechanical stability. Herein, we present a novel strategy to enhance both printability and mechanical strength of a bioink exploiting electrostatic interactions between cationic silica nanoparticles and anionic polysaccharides.

METHODS: Unmodified- (SiNP, -26 mV, 38 nm) and amine-modified (ANP, +29 mV, 41 nm) LUDOX silica nanoparticle dispersion were prepared. Each NP dispersion was added to a polymer mixture comprising two anionic polysaccharides, alginate (Alg)(3 w/v%) and gellan gum (GG)(3.5 w/v%). The mixture was stirred at 90 ^{o}C for 1h followed by vigorous hand-mixing for 15 min at RT. Rheology and compressive modulus were analyzed using a rheometer (MCR 301, Anton Paar) and texture analyzer (TA.XT plus, Stable Micro Systems), respectively. Printing was performed using an extrusion-based 3D printer (Biofactory, RegenHu). Extrusion pressure was kept between 35 – 50 kPa.

RESULTS: Additions of ANP (typically 6 w/v%) resulted in increased viscosity and storage modulus (G') compared with a non-added ink (Alg/GG). The degree of such enhancement affected by several factors. First, compared with SiNP (G' increased by 13%), an addition of ANP resulted in much higher mechanical enhancement (G' increased by 575%, 2700 Pa), which strongly implies that electrostatic interactions between oppositely charged ANP and polysaccharides facilitate great mechanical reinforcement. The storage modulus increased with the concentration of ANP, which reached 3700 Pa with 8 w/v% ANP. In addition, the size of ANP greatly affected the mechanical properties: an addition of large ANP (108 nm) didn't lead to any mechanical

enhancement, whereas the use of smaller ANP (25 nm) resulted in similar mechanical properties with ANP-41nm. After crosslinking in a $CaCl_2$ solution, the storage and compressive modulus of an ANP-ink were increased by 50 % and 61 %, respectively compared with those of an Alg/GG ink. When printing an ear structure with an ANP ink, high structural fidelity was achieved: good printing fidelity was observed during printing, and swelling and shrinkage of a printed construct were greatly suppressed during ionic crosslinking (Fig.1), which were attributed to increased mechanical strength and decreased hydrophilicity of an ANP ink. When a bovine chondrocyte-loaded ANP ink was printed and cultured, the cell viability was found to be 91% at day 21.

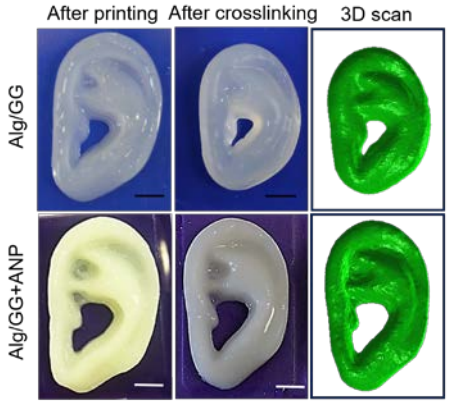

Fig. 1: Photographs of printed ear structures before & after calcium-crosslinking and 3D scanned images of calcium-crosslinked constructs.

CONCLUSIONS: An addition of cationic NP greatly enhanced the mechanical properties of an anionic polymer-based ink and structural fidelity by supressing swelling and shrinkage during ionic crosslinking We expect this new type of bioink formulation involving cationic NPs would contribute to applications of bioprinted tissues where enhanced mechanical properties and high structural fidelity are required.

The influence of primary human intervertebral disc cells on primary human osteoblasts

R.D. May[1], D.A. Frauchiger[1], C.E. Albers[2], L.M. Benneker[2], B. Gantenbein[1]

[1] Tissue and Organ Mechanobiology, Institute for Surgical Technology and Biomechanics, University of Bern, Bern, Switzerland, [2] Department of Orthopaedic Surgery, Inselspital, Bern University Hospital, University of Bern, Bern, Switzerland

INTRODUCTION: Spinal fusion is a common surgical procedure to address a range of spinal pathologies, like damaged or degenerated intervertebral discs (IVD). After the removal of the intervertebral disc, a structural spacer is positioned followed by internal fixation, and fusion of the degenerated segment by natural bone growth. Although spinal fusion is successful in most patients, the rates of non-unions after lumbar spine fusion range from 5 - 35%. Clinical observations and recent studies indicate that the incomplete removal of disc tissue might lead to failure of spinal fusion. Yet, it is still unknown if secretion of BMP antagonists in IVD cells could be the reason of inhibition in bone formation.

METHODS: Osteoblasts (OB) isolated from patients (N = 7) undergoing total knee replacement were seeded at a density of 10'000 cells/cm^2. IVD cells, i.e. nucleus pulposus (NPC), annulus fibrosus (AFC) and cartilaginous endplate cells (CEPC), isolated from patients undergoing spinal surgery. Cell types were separately encapsulated in 1.2 % alginate beads (~ 30 µm in ⌀ at 4M cells/mL, ~ 75'000 cells/bead) and co-cultured via inserts (PET, high density 0.4 µm pore size) with OB in the lower part as monolayer. Six, nine and twelve NPC, AFC or CEPC beads, respectively, were investigated to test the dose response. The experimental groups were stimulated with osteogenic medium. Additionally, we cultured: OB monolayer with osteogenic medium + empty beads as the positive control and OB monolayer with control medium (α-MEM + 10% FCS) as the negative control. Osteoinductive effects in OB were evaluated by Alizarin red staining, Alkaline phosphatase (ALP) activity assay, gene expression of major bone genes and protein level of phosphorylated SMAD 1/5/8. Furthermore, were IVD beads investigated for their bone and IVD marker and BMP antagonist gene expression.

RESULTS: After 21 days, in experimental groups, where OB were stimulated with different numbers of IVD beads, a trend in lower calcium deposition could be observed. Relative gene expression of NPC and CEPC beads is shown in Fig 1.

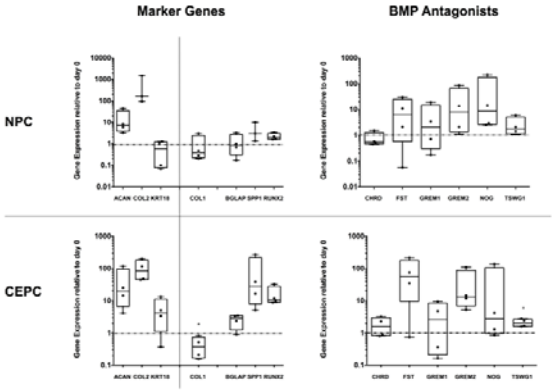

*Fig. 1: Expression of intervertebral disc and major bone marker and BMP antagonist genes in nucleus pulposus (NPC) and cartilaginous endplate cells (CEPC) seeded in alginate beads and cultivated for 21 days in co-culture with human primary osteoblasts and stimulated with osteogenic medium. Gene expression was normalized to day 0 cells of the specific cell type. Significance was tested against day 0 cells. Students t-test, p-value * < 0.05 (N = 4).*

DISCUSSION & CONCLUSIONS: Although we could see a trend in lower matrix mineralization in OB co-cultured with IVD cells, results of ALP activity and gene expression of major bone genes were inconclusive. However, in IVD beads an up-regulation of several BMP antagonist genes could be detected. Despite being able to show several indicators for inhibition of osteoinductive effects due to IVD cells the reasons for pseudarthrosis after spinal fusion remain unclear.

ACKNOWLEDGEMENTS: The project was supported by direct funds from Hansjörg Wyss, the Hansjörg Wyss Medical, US, foundation. C.A. was supported by a grant of the Swiss Orthopaedics Society (SGOT).

Resistance to damage of pre-conditioned composite hydrogel implants

C. Wyss[1], P. Karami[2], A. Khoushabi[1], D. Pioletti[2], P-E. Bourban[1]

[1] Laboratory for Processing of Advanced Composites, [2] Laboratory of Biomechanical Orthopedics , Ecole Polytechnique Fédérale de Lausanne (EPFL), Station 12, CH-1015, Lausanne

INTRODUCTION: Owing to their structure and properties, hydrogels are promising implantable biomaterials to repair or replace some tissues. Indeed, biohydrogel composites can be tailored to mimic the performance of living tissues such as nucleus pulposus and articular cartilages. For clinical applications in load bearing situations, the long-term reliability of hydrogel implants must be known, because mechanical and/or physical properties might change under fatigue loading. For example, conventional double network hydrogels present similar characteristics to the Mullins effect: they become softer after the first loading cycle. Therefore, the long-term behaviour and the evolution of damage of any novel biomaterial need to be thoroughly characterized. In this study, the evolution of the stiffness, fracture properties and microstructure of composite hydrogels were evaluated before, under, and after cyclic loading.

METHODS: Poly (Ethylene Glycol) Dimethacrylate (PEGDM) hydrogels reinforced with different Nano-Fibrillated Cellulose (NFC) fibers and representative neat hydrogels were synthesized. The fatigue behavior of swollen hydrogels were evaluated under cyclic tensile loading. Then single edge crack tests were performed on untreated and treated swollen hydrogels that were previously pre-conditioned under given cyclic loading conditions. In parallel, the open source Digital Image Correlation (DIC) software *ncorr* was used to evaluate how pre-conditioning affects the strain field before and during crack propagation. The 3D microstructure and the failure surfaces were observed with fluorescence confocal microscopy.

RESULTS: The fracture strengths of swollen neat and composite hydrogels are shown on Fig.1 (a), it increases by a factor of 13 when 0.5 wt.% of NFC fibres are added to the PEGDM matrix. However, the elastic modulus of the composite hydrogel is reduced after the first loading cycles before to remain constant, whereas no difference was noticed for the softer neat hydrogel.
Nevertheless, when 50% strain is applied during pre-conditioning, the fracture strength and the crack initiation energy of the composite hydrogel increase by 17% and 27% respectively. DIC analysis, presented on Fig 1(b), reveals that the strain field distribution is affected by the pre-conditioning conditions. In parallel, the microscopy results highlight a gradual reorganisation of the NFC network when the maximal applied strain increases.

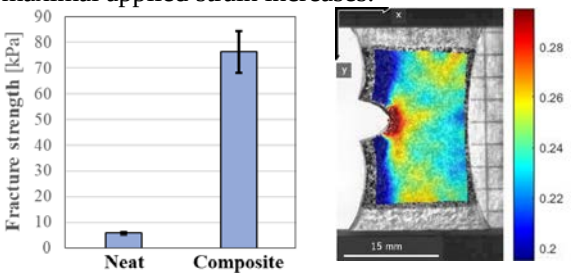

(a) (b)

Fig. 1: (a) Fracture strength of swollen neat and composite hydrogels (b) The Eulerian-Almansi strain field in the y direction of a swollen composite hydrogel during crack propagation.

DISCUSSION & CONCLUSIONS: The study shows that cyclic loading affects the stiffness, the fracture properties and the microstructure of composite hydrogels. The evolution of properties is related to the gradual reorganization of the NFC network. The results demonstrate that the composite hydrogel implant tolerates the induced damage. We hypothesise that pre-conditioning homogenises the stress field at the microscale. Consequently, the stress is better distributed and transferred to the bulk hydrogel, which improves the resistance to crack initiation. Moreover, DIC results suggest that the available volume to dissipate and transform energy affects the tolerance to damage of the composite hydrogel. Hence, depending on the implant dimension, fatigue preloading may have beneficial or detrimental effects on the resistance and tolerance to damage.

ACKNOWLEDGEMENTS: Swiss National Science Foundation, EPFL-BIOP, EPFL-LBO, EPFL-LAPD and EMPA Dübendorf.

Pre-process calculation to optimize laser parameter in selective laser melting

N. Matter[1], F. Schuler[1], R. Schumacher[1], M. de Wild[1]

[1]*Institute for Medical- and Analytical Technologies (IMA), School of Life Sciences FHNW, Muttenz, CH*

INTRODUCTION: Selective Laser Melting (SLM) is an additive manufacturing process, where a laser is used to selectively melt areas in a metallic powder bed. It bears a great potential to produce individual parts of complex geometries, e.g. custom-made implants. To optimize the complex SLM processing throughout the entire component, in-process monitoring and pre-process calculation tools could be used in future. In this work a pre-process calculation was applied to adapt the local laser power during the production of titanium parts.

METHODS: The *RDesigner* Software (DMG MORI) is used to execute the pre-process calculation. The 3D part is sliced into Layer Data and furthermore in cuboid voxels of 100 x 100 x 25 µm^3 (Fig. 1). Based on its topo-logical conditions the algorithm then estimates the thermal connection of each voxel: The laser energy can be absorbed well in red-coloured regions whereas green voxels indicate volumes with low thermal absorption e.g. low heat flow through ambient powder or through the filigree support into the building platform. The aim is to locally reduce the laser energy in these overheated regions according to a predefined function.

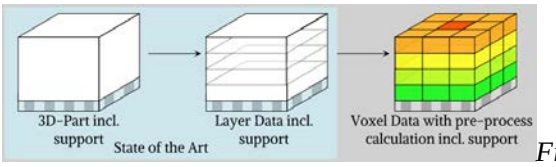

Fig. 1: Estimation of the heat absorption *of each voxel according to its topological situation.*

Mushroom-shaped samples with two different lower cylinder diameter (5 and 10 mm that act as a thermal bottleneck when lasering the massive upper part) were produced out of titanium with the Realizer 125 SLM system (DMG MORI) a) with standard laser parameter (91.5 W) and b) with locally reduced laser energy according to the pre-process calculation.

RESULTS: The results of the pre-process calculation are shown in Fig. 2: Two critical zones were identified and appear green: the connection to the underlying support and the overhanging undersurface. In such overheated areas, the laser power will be dynamically adjusted according to the laser adaption function (Fig. 2c).

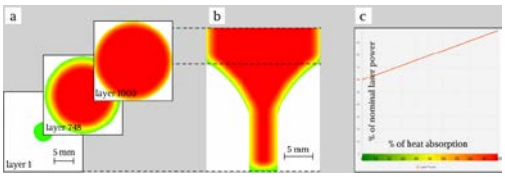

Fig. 2: Result of the pre-process calculation: a) slices at different height, b) frontal plane of the whole sample, c) laser adaption function.

Both parts with 5 mm and 10 mm cylinder diameter could only be completed with the adapted, pre-calculated laser parameter (Fig. 3b). Standard process parameters, however, failed because too much energy was brought in. Therefore, the regions near the overhang superheated because of inadequate heat absorption. Consequently, internal tensions led to deformations. Due to warpage, the building job could not be completed, see Fig. 3a.

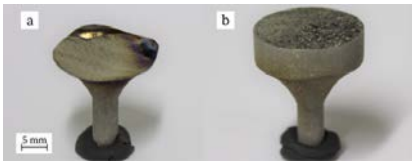

Fig. 3: a) Standard laser parameter: Overheated, incomplete part, b) optimized laser parameter: complete part.

DISCUSSION & CONCLUSIONS: For critical samples with overhangs, thin features such as holes or struts, or large cross-sectional changes, the pre-process calculation can be helpful. The local adjustment of the laser power can increase the quality of the components. However, the definition of the size of the considered topological environment and the precise function of reducing the laser power input remains challenging.

ACKNOWLEDGEMENTS: We thank DMG MORI for their support.

Bioinspired calcium phosphate ceramics: Influence of strontium doping

B. Le Gars Santoni[1], C. Stähli[1], N. Döbelin[1], P. Bowen[2], M. Bohner[1]

[1] *Bioceramics and biocompatibility group, RMS Foundation, Bettlach, CH*

[2] *Laboratory of Powder Technology, Ecole Polytechnique Fédérale de Lausanne, Lausanne, CH*

INTRODUCTION: Calcium phosphates (CaPs) are widely used to improve the self-healing abilities of bone. For decades, dopants (e.g. Sr, Na, Mg…) have been introduced in CaPs in order to modify their physical, chemical and biological properties. However, the incorporation of these dopants during the synthesis by aqueous precipitation may modify the final Ca/P molar ratio of the precipitated calcium deficient hydroxyapatite (CDHA) and thermally treated β-TCP, which is of paramount importance for their *in vivo* behaviour. The aim of this study was to identify a correlation between the dopant concentration, the maturation time of the synthesis, the Ca/P ratio and the unit cell volume of the obtained CaP. Strontium (Sr) a natural impurity encountered in calcium phosphates with anti-osteoporotic properties was selected as a doping agent.

METHODS: The undoped and doped CDHA powders were produced by precipitation in aqueous media. The nominal amounts of the reagents: $(NH_4)_2PO_4$, $Ca(NO_3)_2{\cdot}4H_2O$ and $Sr(NO_3)_2{\cdot}xH_2O$ were used in precise quantities in order to obtain a [Ca+Sr]/[P] molar ratio of 1.5. The CDHA was then left for a maturation time at 30°C. Content of Sr in CDHA was analysed by ICP-MS and its specific surface area (SSA) was measured by BET. Phase purity and unit cell volume were determined by XRD after thermal conversion of CDHA into crystalline β-TCP.

RESULTS: The effects of Sr on unit cell volume, Ca/P ratio and SSA are summarized in (Fig 1.a). The higher was the Sr content, the higher was the β-TCP unit cell volume ($p < 1{\cdot}10^{-6}$).

a

	ICP-MS (on CDHA)	BET (on CDHA)	XRD (on β-TCP)	
CDHA powder name	Sr Content [ppm]	SSA [m²/g]	[Ca+Sr]/P molar ratio [-]	Unit cell volume [Å³]
CDHA pure (n=7)	262 ± 70	108 ± 6	1.50 ± 0.01	3530.35 ± 0.72
CDHA 1 % Sr (n=4)	7999 ± 398	102 ± 17	1.49 ± 0.01	3532.32 ± 0.32
CDHA 1.71 % Sr (n=3)	13773 ± 524	103 ± 7	1.49 ± 0.01	3534.03 ± 0.50
CDHA 2.92 % Sr (n=4)	23717 ± 698	106 ± 12	1.49 ± 0.01	3536.48 ± 0.36
CDHA 5 % Sr (n=3)	40109 ± 1000	105 ± 5	1.48 ± 0.01	3541.96 ± 0.57

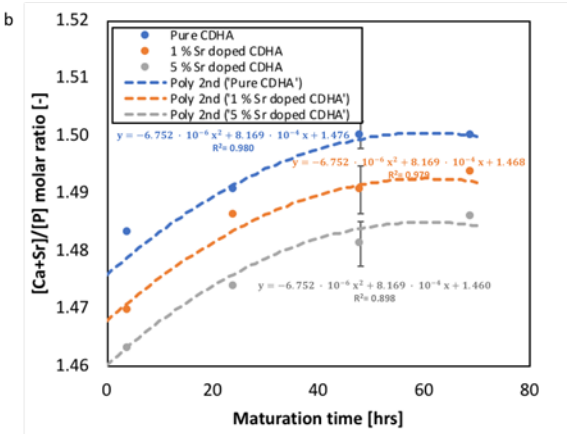

Fig. 1: (a) Characteristics of undoped and doped CDHA and β-TCP powders. (b) Effect of the maturation time, dopant concentration on the Ca/P molar ratio of β-TCP powders.

Moreover, the higher was the Sr concentration, the lower was the [Ca+Sr]/[P] ratio ($p < 1{\cdot}10^{-4}$).

DISCUSSION & CONCLUSIONS: This study highlighted how the presence of Sr doping can affect the Ca/P ratio and the unit cell volume of the synthetized and thermally treated β-TCP. Specifically, the higher was the Sr concentration, the lower was the [Ca+Sr]/[P] ratio and the higher was the β-TCP unit cell volume. The maturation time of the synthesis was found to increase the [Ca+Sr]/[P] ratio of both undoped and doped β-TCP but had no influence on the unit cell volume meaning that the maturation time had no influence on the Sr content in β-TCP (results not shown here). With highly doped β-TCP, a [Ca+Sr]/[P] ratio of 1.5, could not be reached. Since the density and the grain size of the β-TCP cylinders obtained after sintering from CDHA powders are highly influenced by the [Ca+Sr]/[P] ratio (results not shown here), future synthesis will be done by increasing temperature or pH to reach within an acceptable maturation time the [Ca+Sr]/[P] ratio of 1.5.

ACKNOWLEDGEMENTS: This work was funded by the Swiss National Science Foundation grant 200021_169027

Are humanized mice a good animal model for cartilage tissue engineering? A comparative study of chondrogenesis under varying immune backgrounds

E. Cavalli[1, §], P. Fisch[1, §], F. Formica[1], R. Galreus[2], L. A. Applegate[3], M. Zenobi-Wong[1]

[1] *Tissue Engineering and Biofabrication, ETH Zürich, CH.* [2] *The Jackson Laboratory, USA.*
[3] *Musculoskeletal Medicine, University Hospital Lausanne, CH.* [§] *equal contribution*

INTRODUCTION: *In vivo* testing plays a pivotal role in tissue engineering and animal models remain fundamental to many aspects of both basic and translational studies. Due to the high number of scientific and ethical considerations, choosing the right model for the assessment of new biomaterial-based strategies for cartilage repair is a challenge. Despite the widespread use of immunodeficient mice for subcutaneous implantation of engineered cartilage constructs, there is no consensus on whether these animals are the optimal choice. Furthermore, the development of humanized mice have raised the question of whether these chimeras would represent an alternative animal model for the field.

The aim of this study was to evaluate and compare the chondrogenic potential of a novel, tissue engineered construct for cartilage repair applications in 4 different mouse strains, namely NSG, nude, NSG-SGM3 humanized and C57B6 The biomaterial, namely HA-TG, used is a hyaluronic acid (HA) based hydrogel produced by substituting the hyaluronan backbone with transglutaminase (TG) crosslinkable peptides. The scaffold was investigated acellular and combined with one of two cell types of different origins: juvenile human auricular chondrocytes (hAUR) and human fetal chondroprogenitor cells (hCCs).

METHODS: HA-TG precursors were synthetized as previously described. Cylindrical gels (d=4mm, h=2mm) were casted acellular and cell-laden with either hAURs or hCCs. After 4 weeks of preculture *in vitro*, the scaffolds were implanted subcutaneously in the back of the 4 mouse strains and maintained for 4 additional weeks. Gel volume and vascularization were analysed with an ultrasound/photoacoustic device *in vivo*. At euthanization blood samples were collected and further analysed for inflammation markers (CRP, SAA, SAP). Explanted scaffolds were tested for mechanical properties under compression and histologically stained for collagen II, collagen I, macrophages (CD68) and anti-inflammatory macrophages (CD163).

	Mouse Strain	Black 6	Nude	Humanized	NSG
Innate Immune System	Hemolytic Complement	✔	✔	✗	✗
	Granulocytes	✔	✔	✔ CD33+	✔
	Natural Killer Cells	✔	✔	✔	✗
	Macrophages	✔	✔	Some functional CD33+	defective
Adaptive Immune System	T Lymphocytes	✔	✗	✔ human	✗
	B Lymphocytes	✔	✔	Some functional human	✗
	Antibodies	✔	✔	low production of IgG	✗
	Dendritic Cells	✔	✗	Some functional CD33+	defective

Fig. 1: Immune system differences in the mouse strains used in the study.

RESULTS: HA-TG constructs were able to maintain their volumes and resist vascularization for up to 4 weeks *in vivo*. For all mouse strains a significantly higher deposition of collagen II was observed in the hAUR encapsulated scaffolds. No statistically significant difference in mechanical properties was observed among the strains.
CRP levels were elevated in black 6 mice while acute inflammation phase markers SAA and SAP were lower in NSG mice. Both CD68+ and CD163+ macrophages were highly present around the scaffolds implanted in black 6 mice.

DISCUSSION & CONCLUSIONS: While hAURs performed consistently better than hCCs in maintaining and producing cartilaginous ECM *in vivo*, chondrogenesis and inflammation were comparable between mouse strains. The results suggest that the mouse immune system might play a less fundamental role in subcutaneous studies of cartilage engineered constructs than previously hypothesized.

ACKNOWLEDGEMENTS: This work was supported by the ETH Zurich Foundation (Grant No. ETH-50 13-1) and a CABMM startup grant.